Canard Cycles and Homoclinic Orbit of a Leslie–Gower Predator–Prey Model with Allee Effect and Holling Type II Functional Response

Tianyu Shi[1] · Zhenshu Wen[1]

Abstract

We study dynamics of a fast–slow Leslie–Gower predator–prey system with Allee effect and Holling Type II functional response. More specifically, we show some sufficient conditions to guarantee the existence of two positive equilibria of the system and their location, and then we further fully determine their dynamics. Based on geometric singular perturbation theory and the slow–fast normal form, we determine the associated bifurcation curve and observe canard explosion. Besides, we also find a homoclinic orbit to a saddle with slow and fast segments, in which, the stable and unstable manifolds of the saddle are connected under explicit parameters conditions.

Keywords Canard cycle · Homoclinic orbit · Geometric singular perturbation theory

Mathematics Subject Classification 34C07 · 34D15 · 34E15 · 37G15

1 Introduction

The complexity of ecological dynamics has been a challenging field for mathematical and theoretical ecologists for several decades. As an elementary building block for many interesting population models, the predator–prey models have attracted considerate interest and remain to be research focus. As we know, the classical Leslie–Gower predator–prey model [1, 2] can be described as follows:

✉ Zhenshu Wen
wenzhenshu@hqu.edu.cn

1 School of Mathematical Sciences, Huaqiao University, Quanzhou 362021, People's Republic of China

$$\begin{cases} \frac{dx}{dt} = rx\left(1 - \frac{x}{K}\right) - p(x)y, \\ \frac{dy}{dt} = sy(1 - \frac{y}{hx}), \end{cases} \tag{1}$$

where x and y denote population density of prey and predator at time t, respectively, $p(x)$ is the functional response, and other parameters r, s, K and h are all positive which have corresponding biological meanings: r and s stand for the intrinsic growth rates of prey and predator, respectively, K indicates the prey environment carrying capacity, and h represents the quality of the prey as food for the predator. The term $\frac{y}{x}$ is the Leslie–Gower term which measures the loss in the predator population due to rarity of its favorite food. In the classical Leslie–Gower model, the carrying capacity of the predator is proportional to the number of prey, stressing the fact that there are upper limits to the rates of increase in both prey and predator, which are not recognized in the Lotka–Volterra model. There has been great interest in studying dynamics of the classical Leslie–Gower model and its variants. Hsu and Huang [3, 4] dealt with limit cycle, Hopf bifurcation, and global stability of the positive locally asymptotically stable equilibrium about system (1). Korobeinikov [5] introduced a Lyapunov function and established global stability of the unique coexisting equilibrium state of Leslie–Gower predator–prey models. Yuan and Song [6] focused on bifurcation and stability of a delayed Leslie–Gower predator–prey system. As we know, one important feature of the prey–predator relationship is the rate of prey consumption by an average consumer (predator), i.e., functional response. The effects of different functional responses (Holling type I, II, III, IV, and so on) on the dynamics of the predator–prey models have been investigated to a great extent [7]. Huang et al. [8] and Dai et al. [9] concentrated on dynamics of a Leslie–Gower predator–prey model with generalized Holling type III functional response. Tripathi et al. [10–13] dealt with rich dynamics of Leslie–Gower predator–prey models with Beddington–DeAngelis functional response. It is well–known that Allee effect [14], which reflects the relation between population size and fitness, is also a critical factor in characterizing species diversity maintenance, species evolution, species conservation and management in ecological research. Therefore, much effort has been made to study the dynamics of the predator–prey models with Allee effect [15]. For instance, Aguirre et al. [16, 17] studied system (1) with the additive Allee effect

$$\begin{cases} \frac{dx}{dt} = rx(1 - \frac{x}{K} - \frac{m}{x+b}) - p(x)y, \\ \frac{dy}{dt} = sy(1 - \frac{y}{hx}), \end{cases}$$

where m and b are positive constants that indicate the severity of the Allee effect, and Aguirre [18] also focused on system (1) with the multiplicative Allee effect

$$\begin{cases} \frac{dx}{dt} = rx(1 - \frac{x}{K})(x - m) - p(x)y, \\ \frac{dy}{dt} = sy(1 - \frac{y}{hx}), \end{cases}$$

where m is the Allee threshold of viable population.

Zhu et al. [19] considered system (1) with another form of Allee effect (indicating that the intrinsic growth rate of the prey depends on the population size) and Holling Type I functional response $p(x) = ex$,

$$
\begin{cases}
\frac{dx}{dt} = x\left(\frac{rx}{x+a} - bx - c\right) - exy, \\
\frac{dy}{dt} = sy(1 - \frac{y}{hx}),
\end{cases}
\tag{2}
$$

where $a > 0$ is the Allee effect constant of the prey, $c > 0$ is the mortality of the prey, $b > 0$ is the intra–specific competition intensity of the prey, and $e > 0$ represents the maximal predator per capita consumption rate. Zhu et al. [19] studied the existence and stability of equilibria, and then showed that system (2) undergoes Bogdanov–Takens bifurcation of codimension two (or three). Zu and Mimura [20] found that this type of Allee effect can increase the risk of extinction of both predator and prey by including Allee effect and Holling Type II functional response. They [20, 21] also showed that the model can undergo the heteroclinic loop bifurcation and Hopf bifurcation. In this paper, we concentrate on the dynamics of the slow–fast version of the following system with Allee effect and Holling Type II functional response $p(x) = \frac{ex}{d+x}$,

$$
\begin{cases}
\frac{dx}{dt} = x\left(\frac{rx}{x+a} - bx - c\right) - \frac{exy}{d+x}, \\
\frac{dy}{dt} = sy(1 - \frac{y}{hx}).
\end{cases}
\tag{3}
$$

It is believed that ecological systems in nature usually evolve on different time scales. Therefore, considering the fact that the growth of the prey and its predator occurs on different time scales, many researchers have devoted to studying the dynamics of the fast–slow predator–prey models [22–32]. Wang et al. [22, 23] studied dynamics of a slow–fast predator–prey model with the generalized Holling type III functional response. Chen and Zhang [24] studied canard explosion of a slow–fast predator–prey model with the Sigmoid functional response. Atabaigi [25] analyzed dynamics of a slow–fast generalist predator–prey model with Holling type III functional response. Saha et al. [26] investigated dynamics of a slow–fast modified Leslie–type prey–generalist predator system with piecewise-smooth Holling type I functional response. Zhu and Liu [27] investigated canard cycles and relaxation oscillation in a slow–fast predator–prey model with the generalized Holling type II functional response and Allee effect. Zhao and Shen [28] focused on canards and homoclinic orbits of a slow–fast modified May–Holling–Tanner predator–prey model with weak multiple Allee effect. Shi and Wen [29] investigated canard cycles and their cyclicity of the slow–fast version of system (2). Chowdhury, Banerjee and Petrovskii [30] studied canards, relaxation oscillations, and pattern formation in a slow–fast ratio–dependent predator–prey model. Li et al. [31] concentrated on relaxation oscillation and canard explosion in a slow–fast predator–prey model with Holling type I functional response and addictive Allee effect. Wen and Shi [32] proved the existence and uniqueness of a canard cycle with cyclicity at most two in a singularly perturbed Leslie–Gower predator–prey model with prey harvesting. With these great success, one may wander what about the dynamics in the slow–fast version of system (3). Motivated by this,

by assuming that prey reproduces much faster than predator, that is, $\varepsilon = s/r \ll 1$, exploiting the transformation

$$x = \frac{r}{b}\bar{x},\, y = \frac{r^2}{be}\bar{y},\, t = \frac{t_1}{r},$$

and dropping the bars, we rewrite system (3) into

$$\begin{cases} \frac{dx}{dt_1} = x\left(\frac{x}{A+x} - \alpha - x - \frac{y}{\beta+x}\right), \\ \frac{dy}{dt_1} = \varepsilon y\left(1 - \frac{ky}{x}\right), \end{cases} \tag{4}$$

where $A = \frac{ab}{r}$, $\alpha = \frac{c}{r}$, $\beta = \frac{bd}{r}$, and $k = \frac{r}{eh}$. Note that A in system (4) corresponds to Allee effect constant a in system (3).

Obviously, system (4) is topologically equivalent to

$$\begin{cases} \frac{dx}{dt} = x^2\Big((x - (\alpha+x)(A+x))(\beta+x) - y(A+x)\Big), \\ \frac{dy}{dt} = \varepsilon y(A+x)(\beta+x)(x - ky). \end{cases} \tag{5}$$

From the perspective of geometric singular perturbation theory (GSPT), system (5) is called the fast system. We are going to study dynamics of system (5), including canard explosion and homoclinic orbit.

2 Preliminaries

In this section, to study the dynamics of system (5), we first give some preliminary results, based on geometric singular perturbation theory [33] and the slow–fast normal form [34].

2.1 The Slow and Fast Limiting Dynamics

Introducing $\tau = \varepsilon t$, we obtain the associated slow system of system (5)

$$\begin{cases} \varepsilon\frac{dx}{d\tau} = x^2\Big((x - (\alpha+x)(A+x))(\beta+x) - y(A+x)\Big), \\ \frac{dy}{d\tau} = y(A+x)(\beta+x)(x - ky). \end{cases} \tag{6}$$

Setting $\varepsilon = 0$ in systems (5) and (6), we arrive at the fast subsystem

$$\begin{cases} \frac{dx}{dt} = x^2\Big((x - (\alpha+x)(A+x))(\beta+x) - y(A+x)\Big), \\ \frac{dy}{dt} = 0, \end{cases} \tag{7}$$

and the slow subsystem

$$\begin{cases} 0 = x^2\Big((x - (\alpha + x)(A + x))(\beta + x) - y(A + x)\Big), \\ \frac{dy}{d\tau} = y(A + x)(\beta + x)(x - ky), \end{cases} \tag{8}$$

respectively. According to GSPT, our aim is to study dynamics of system (5) by combining the limiting information of systems (7) and (8).

2.2 The Critical Manifold

It follows that the critical manifold of system (8) is given by

$$C_0 = \{(x, y)|x = 0\} \cup \{(x, y)|y = C(x)\} := C_1 \cup C_2, \tag{9}$$

where

$$C(x) = (\beta + x)\left(\frac{x}{A + x} - \alpha - x\right). \tag{10}$$

To state conveniently, throughout the remainder of the paper, we always assume that

$$0 < A < 1 \text{ and } 0 < \alpha < \left(1 - \sqrt{A}\right)^2. \tag{11}$$

Then we easily find that the critical manifold C_2 has a unique fold point $Q(x_Q, y_Q)$, where $y_Q = C(x_Q)$. Besides, one also notice that $y = C(x)$ intersects the x–axis at two points $E_{b1}(x_{b1}, 0)$ and $E_{b2}(x_{b2}, 0)$, where

$$x_{b1} = \frac{1}{2}\left(1 - A - \alpha - \sqrt{(1 - \alpha - A)^2 - 4A\alpha}\right) \text{ and}$$
$$x_{b2} = \frac{1}{2}\left(1 - A - \alpha + \sqrt{(1 - \alpha - A)^2 - 4A\alpha}\right).$$

Hence the critical manifold C_2 can be divided into the following two parts by the point Q

$$C_2^r = \{(x, y)|y = C(x), x_{b1} < x < x_Q\} \text{ and } C_2^a = \{(x, y)|y = C(x), x_Q < x < x_{b2}\}. \tag{12}$$

According to GSPT, one immediately has the following results.

Lemma 1 *One has,*

(i) *C_2^r is normally hyperbolic repelling; and C_2^a is normally hyperbolic attracting.*
(ii) *C_2^r and C_2^a perturb to nearby invariant manifolds $C_{2,\varepsilon}^r$ and $C_{2,\varepsilon}^a$, respectively.*

2.3 Equilibria and their Dynamics

One first easily notices that the set $\Omega = \{(x, y)|0 < x < x_{b2}, y \geq 0\}$ is positively invariant and is attracting with respect to the flow of system (5). Additionally, one also has the following results by direct calculation.

Lemma 2 *System (5) has two boundary equilibria E_{b1} and E_{b2} with $0 < A < 1$ and $0 < \alpha < \left(1 - \sqrt{A}\right)^2$. Furthermore, E_{b1} is a saddle and E_{b2} is an unstable node.*

Next, we turn to positive equilibria of system (5). Cleary, the abscissa of positive equilibria should satisfy

$$kx^3 + \left(k(\alpha + A + \beta - 1) + 1\right)x^2 + \left(\beta k(\alpha + A - 1) + A(\alpha k + 1)\right)x + \alpha A \beta k = 0.$$
$$(13)$$

Let

$$
\begin{aligned}
\Delta_1 &= (k(\alpha + A + \beta - 1) + 1)^2 - 3k\left(\beta k(\alpha + A - 1) + A(\alpha k + 1)\right), \\
\Delta_2 &= -27k^3\alpha A\beta + 9k\left(k(\alpha + A + \beta - 1) + 1\right)\left(\beta k(\alpha + A - 1) + A(\alpha k + 1)\right) \\
&\quad + 2\left(k(\alpha + A + \beta - 1) + 1\right)^3.
\end{aligned}
$$

Now we can state the results about the number, position and dynamics of positive equilibria of system (5).

Theorem 1 *If $0 < \varepsilon \ll 1$, $0 < A < 1$, and $0 < \alpha < \left(1 - \sqrt{A}\right)^2$, $\Delta_2^2 - 4\Delta_1^3 < 0$, and $\sqrt{\Delta_1} - k(\alpha + A + \beta - 1) - 1 > 0$, then system (5) has two positive equilibria $E_1(x_1, y_1)$ and $E_2(x_2, y_2)$ with $x_{b1} < x_2 < x_1 < x_{b2}$. Additionally, E_2 is saddle, and*

(i) *if $k < \frac{x_Q}{y_Q}$, then $x_2 < x_1 < x_Q$. Moreover, if $k < \frac{x_Q}{y_Q}$ and k is not sufficiently close to $\frac{x_Q}{y_Q}$, then E_1 is unstable node.*
(ii) *if $k = \frac{x_Q}{y_Q}$, then $x_2 < x_1 = x_Q$. Moreover, E_1 is stable focus.*
(iii) *if $k > \frac{x_Q}{y_Q}$, then $x_2 < x_Q < x_1$. Moreover, if $k > \frac{x_Q}{y_Q}$ and k is not sufficiently close to $\frac{x_Q}{y_Q}$, then E_1 is stable node.*

Proof The statements about the existence of two positive equilibria and their location follow from direct calculation. To study the dynamical behavior of the positive equilibrium (x, y), we find the Jacobian matrix of system (5) at the equilibrium (x, y)

$$J(x, y) = \begin{bmatrix} x^2\left((\beta + x)(1 - \alpha - A - 2x) - (A + x)(\alpha + x) + x - y\right) & -x^2(A + x) \\ \varepsilon y(\beta + x)(A + x) & -\varepsilon ky(\beta + x)(A + x) \end{bmatrix}.$$

Clearly, its trace $Tr(J(x, y))$ and determinant $Det(J(x, y))$ are given by

$$Tr(J(x, y)) = x^2(A + x)\left(\frac{x}{A + x} - x - \alpha + \frac{\left(A - (A + x)^2\right)(\beta + x)}{(A + x)^2}\right)$$
$$- \varepsilon x(\beta + x)(A + x)$$
$$= x^2(A + x)C'(x) - \varepsilon x(\beta + x)(A + x),$$

and

$$Det(J(x, y)) = \varepsilon x^2 y(\beta + x)(A + x)\Big(3kx^2 + 2(k(\alpha + A + \beta - 1) + 1)x$$
$$+ \big(\beta k(\alpha + A - 1) + A(\alpha k + 1)\big)\Big)$$
$$= -\varepsilon x^2 y(\beta + x)(A + x)H'(x),$$

respectively.

Obviously, one has, for the equilibrium E_2 if exists, $Det(J(x_2, y_2)) = -\varepsilon x_2^2 y_2(\beta + x_2)(A + x_2)H'(x_2) < 0$ and $Tr^2(J(x_2, y_2)) - 4Det(J(x_2, y_2)) > 0$, which implies that E_2 is saddle. While, for the equilibrium E_1, $Det(J(x_1, y_1)) = -\varepsilon x_1^2 y_1(\beta + x_1)(A + x_1)H'(x_1) > 0$ and $Tr^2(J(x_1, y_1)) - 4Det(J(x_1, y_1)) > 0$ (resp. $Tr^2(J(x_1, y_1)) - 4Det(J(x_1, y_1)) < 0$) for sufficiently small $\varepsilon > 0$ if $x_1 \neq x_Q$ and x_1 is not sufficiently close to x_Q (resp. $x_1 = x_Q$). Besides, one also has, if $x_1 < x_Q$ (resp. $x_1 > x_Q$) and x_1 is not sufficiently close to x_Q, then $Tr(J(x_1, y_1)) > 0$ (resp. $Tr(J(x_1, y_1)) < 0$) for sufficiently small $\varepsilon > 0$, and if $x_1 = x_Q$, then $Tr(J(x_1, y_1)) = -\varepsilon x_1 (\beta + x_1)(A + x_1) < 0$. Additionally, one also notices that if k is not sufficiently close to $\frac{x_Q}{y_Q}$, then x_1 is not sufficiently close to x_Q. Hence, the dynamical behavior of E_1 follows. □

Remark 1 One can also determine the number, stability and topological types of positive equilibria through analyzing fast dynamics and slow dynamics along C_2 (see [35, 36] for details).

Taking $\epsilon = 0.0005$, $A = 0.4$, $\alpha = 0.05$, and $\beta = 1.8$, here we illustrate the phase portraits and types of positive equilibria E_1 and E_2 in Fig. 1a–c when $k = 1.1$, $k = 1.417692643$, and $k = 3$, respectively, which satisfy corresponding conditions given in (i), (ii), and (iii) of Theorem 1.

2.4 Slow–Fast Normal Form

From Theorem 1, we know that when $k = \frac{x_Q}{y_Q}$, the fold point $Q(x_Q, y_Q)$ is also an equilibrium point of system (5), that is, $x_Q = x_1$, and it is easy to verify that Q is a non–degenerate canard point [34] of system (5).
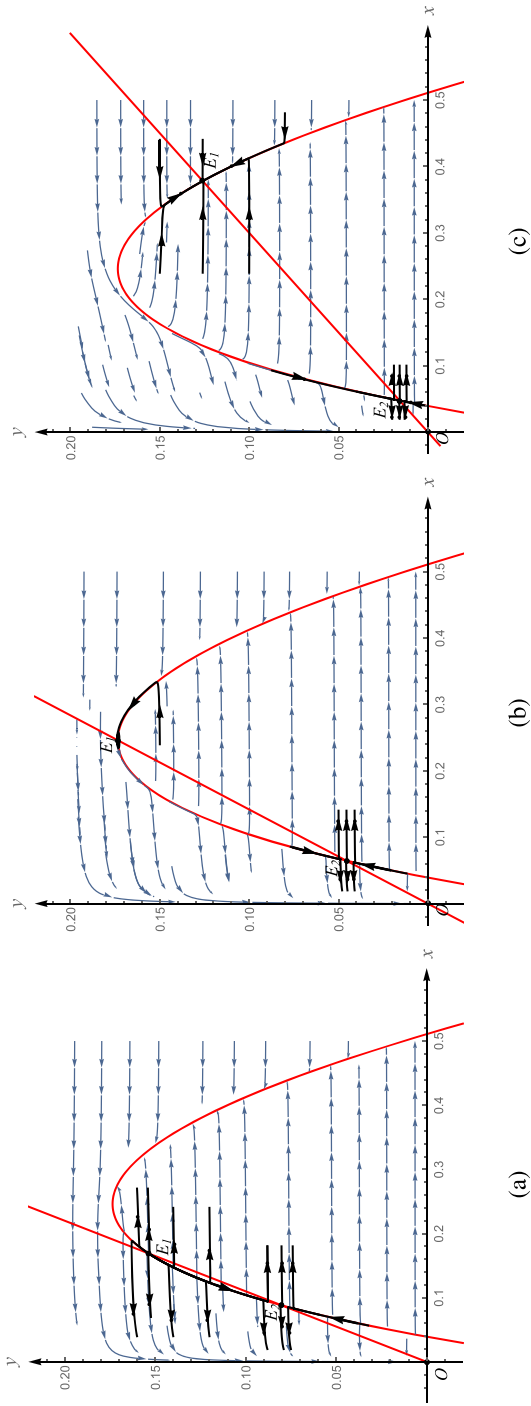
Fig. 1 Illustrations of saddle E_2 and **a** unstable node E_1; **b** stable focus E_1; **c** stable node E_1

Now we transform system (5) into its slow–fast normal form given in [34]. To get started, let $T = x^2 (A + x) t$, and then system (5) can be written as

$$
\begin{cases}
\frac{dx}{dT} = -y + (\beta + x)\left(\frac{x}{A+x} - \alpha - x\right), \\
\frac{dy}{dT} = \varepsilon \frac{y(\beta+x)}{x}\left(1 - \frac{ky}{x}\right).
\end{cases}
\tag{14}
$$

Then we move the point (x_Q, y_Q) to the origin through $X = x - x_Q$, $Y = y - y_Q$, and system (14) becomes

$$
\begin{cases}
\frac{dX}{dT} = -Y + \left(\frac{A(A-\beta)}{(A+x_Q)^3} - 1\right) X^2 + \frac{A(\beta-A)}{(A+x_Q)^4} X^3 + O(X^4), \\
\frac{dY}{dT} = \varepsilon \left(a_{00} + a_{10} X + a_{20} X^2 + (a_{01} + a_{11} X + a_{02} Y) Y + O(|X, Y|^3)\right),
\end{cases}
\tag{15}
$$

where

$$
a_{00} = \frac{y_Q(\beta + x_Q)(x_Q - ky_Q)}{x_Q^2}, \quad a_{10} = \frac{\beta y_Q(2ky_Q - x_Q) + kx_Q y_Q^2}{x_Q^3},
$$

$$
a_{20} = \frac{\beta y_Q(x_Q - 3ky_Q) - kx_Q y_Q^2}{x_Q^4},
$$

$$
a_{01} = \frac{(\beta + x_Q)(x_Q - 2ky_Q)}{x_Q^2}, \quad a_{11} = \frac{(2kx_Q y_Q + 4\beta ky_Q - \beta x_Q)}{x_Q^3}, \quad a_{02} = -\frac{k(\beta + x_Q)}{x_Q^2}.
$$

Further employing the transformation $X = -\frac{(A+x_Q)\sqrt{y_Q(ky_Q(2\beta+x_Q)-\beta x_Q)}}{x_Q^{3/2}(\alpha+A+\beta+3x_Q-1)} X_1$, $Y = -\frac{y_Q(A+x_Q)(ky_Q(2\beta+x_Q)-\beta x_Q)}{x_Q^3(\alpha+A+\beta+3x_Q-1)} Y_1$, $T = \frac{x_Q^{3/2}}{\sqrt{y_Q(ky_Q(2\beta+x_Q)-\beta x_Q)}} T_1$, we convert system (15) into the slow–fast normal form

$$
\begin{cases}
\frac{dX_1}{dT_1} = -Y_1 h_1(X_1, Y_1, \lambda, \varepsilon) + X_1^2 h_2(X_1, Y_1, \lambda, \varepsilon) + \varepsilon h_3(X_1, Y_1, \lambda, \varepsilon), \\
\frac{dY_1}{dT_1} = \varepsilon \left(X_1 h_4(X_1, Y_1, \lambda, \varepsilon) - \lambda h_5(X_1, Y_1, \lambda, \varepsilon) + Y_1 h_6(X_1, Y_1, \lambda, \varepsilon)\right),
\end{cases}
\tag{16}
$$

where

$$
\lambda = \frac{x_Q^{5/2}(\beta + x_Q)(x_Q - ky_Q)(\alpha + A + \beta + 3x_Q - 1)}{\sqrt{y_Q}(A + x_Q)(ky_Q(2\beta + x_Q) - \beta x_Q)^{3/2}},
$$

$$
h_1(X_1, Y_1, \lambda, \varepsilon) = 1,
$$

$$
h_2(X_1, Y_1, \lambda, \varepsilon) = 1 + \frac{(\alpha + \beta + 2x_Q - 1)\sqrt{y_Q(ky_Q(2\beta + x_Q) - \beta x_Q)}}{x_Q^{3/2}(\alpha + A + \beta + 3x_Q - 1)^2} X_1 + O(X_1^2),
$$

$$
h_3(X_1, Y_1, \lambda, \varepsilon) = 0,
$$

$$
h_4(X_1, Y_1, \lambda, \varepsilon) = 1 + \frac{\sqrt{y_Q}(A + x_Q)(ky_Q(3\beta + x_Q) - \beta x_Q)}{x_Q^{5/2}(\alpha + A + \beta + 3x_Q - 1)\sqrt{ky_Q(2\beta + x_Q) - \beta x_Q}} X_1 + O(X_1^2),
$$

$$
h_5(X_1, Y_1, \lambda, \varepsilon) = 1,
$$

$$h_6(X_1, Y_1, \lambda, \varepsilon) = \frac{(\beta + x_Q)(x_Q - 2ky_Q)}{\sqrt{x_Q}\sqrt{y_Q(ky_Q(2\beta + x_Q) - \beta x_Q)}} + O(X_1, Y_1). \tag{17}$$

Note that

$$\lambda = 0 \Leftrightarrow k = \frac{x_Q}{y_Q}. \tag{18}$$

Therefore, we have

$$a_1 = \frac{\partial h_3}{\partial X_1}(0, 0, 0, 0) = 0, \ a_2 = \frac{\partial h_1}{\partial X_1}(0, 0, 0, 0) = 0,$$

$$a_3 = \frac{(\alpha + \beta + 2x_Q - 1)\sqrt{y_Q(\beta + x_Q)}}{x_Q(\alpha + A + \beta + 3x_Q - 1)^2},$$

$$a_4 = \frac{\sqrt{y_Q}(A + x_Q)(2\beta + x_Q)}{x_Q^2\sqrt{\beta + x_Q}(\alpha + A + \beta + 3x_Q - 1)}, \ a_5 = h_6(0, 0, 0, 0) = -\frac{\sqrt{\beta + x_Q}}{\sqrt{y_Q}}, \tag{19}$$

and further

$$B = -a_2 + 3a_3 - 2a_4 - 2a_5$$

$$= \frac{1}{x_Q^2\sqrt{y_Q(\beta + x_Q)}(\alpha + A + \beta + 3x_Q - 1)^2}\left(18x_Q^5 + 6x_Q^4(2(\alpha + A - 1) + 5\beta)\right.$$

$$+ 2x_Q^3(\alpha + A + \beta - 1)(\alpha + A + 7\beta - 1) + x_Q^2\left(2\beta(\alpha + A + \beta - 1)^2\right.$$

$$+ y_Q(\alpha - 8A - 5\beta - 1))$$

$$\left. - x_Q y_Q\left(\beta(\alpha + 18A - 1) + 2A(\alpha + A - 1) + \beta^2\right) - 4A\beta y_Q(\alpha + A + \beta - 1)\right). \tag{20}$$

Hence the singular Hopf bifurcation curve and the maximal canard curve of the slow–fast normal form (16) are given by

$$\lambda_H(\sqrt{\varepsilon}) = -\frac{a_1 + a_5}{2}\varepsilon + O(\varepsilon^{\frac{3}{2}}) = \frac{\sqrt{\beta + x_Q}}{2\sqrt{y_Q}}\varepsilon + O(\varepsilon^{\frac{3}{2}}), \tag{21}$$

and

$$\lambda_c(\sqrt{\varepsilon}) = -\left(\frac{a_1 + a_5}{2} + \frac{1}{8}B\right)\varepsilon + O(\varepsilon^{\frac{3}{2}})$$

$$= \frac{1}{8x_Q^2\sqrt{y_Q(\beta + x_Q)}(\alpha + A + \beta + 3x_Q - 1)^2}\left(18x_Q^5 + 6x_Q^4(2(\alpha + A - 1)\right.$$

$$+ 5\beta) + 2x_Q^3(\alpha + A + \beta - 1)(\alpha + A + 7\beta - 1)$$

$$+ x_Q^2\left(2\beta(\alpha + A + \beta - 1)^2 + y_Q(-\alpha + 8A + 5\beta + 1)\right)$$

$$+ x_Q y_Q\left(\beta(\alpha + 18A - 1) + 2A(\alpha + A - 1) + \beta^2\right)$$

$$+ 4A\beta y_Q(\alpha + A + \beta - 1)\Big)\varepsilon + O(\varepsilon^{\frac{3}{2}}), \tag{22}$$

respectively.

Correspondingly, the singular Hopf bifurcation curve and the maximal canard curve of system (5) can be expressed as, respectively

$$k_H(\sqrt{\varepsilon}) = \frac{x_Q}{y_Q} - \frac{A + x_Q}{2\sqrt{\beta + x_Q}(2\beta + x_Q)^{\frac{3}{2}}\left(x_Q y_Q\right)^{\frac{5}{2}}(\alpha + A + \beta + 3x_Q - 1)}\varepsilon + O(\varepsilon^{\frac{3}{2}}), \tag{23}$$

and

$$k_c(\sqrt{\varepsilon}) = \frac{x_Q}{y_Q} - \frac{A + x_Q}{8\Big((\beta + x_Q)(2\beta + x_Q)\Big)^{\frac{3}{2}} x_Q^{\frac{7}{2}} y_Q^{\frac{5}{2}}(\alpha + A + \beta + 3x_Q - 1)^3}$$

$$\left(18x_Q^5 + 6x_Q^4(2(\alpha + A - 1) + 5\beta)\right.$$

$$+ 2x_Q^3(\alpha + A + \beta - 1)(\alpha + A + 7\beta - 1)$$

$$+ x_Q^2\left(2\beta(\alpha + A + \beta - 1)^2 + y_Q(-\alpha + 8A + 5\beta + 1)\right)$$

$$+ x_Q y_Q\left(\beta(\alpha + 18A - 1) + 2A(\alpha + A - 1) + \beta^2\right)$$

$$+ 4A\beta y_Q(\alpha + A + \beta - 1)\Bigg)\varepsilon + O(\varepsilon^{\frac{3}{2}}). \tag{24}$$

3 Canard Cycles and Homoclinic Orbit of the Slow–Fast System (5)

In this section, we focus on canard cycles and homoclinic orbit of the slow–fast system (5). From Theorem 1, we know when $0 < A < 1$, $0 < \alpha < \left(1 - \sqrt{A}\right)^2$, and $k = \frac{x_Q}{y_Q}$, the positive equilibrium E_1 of system (5) coincides with Q and the other positive equilibrium E_2 is saddle of system (5).

Theorem 2 *Assume that $0 < \varepsilon \ll 1$, $0 < A < 1$, and $0 < \alpha < \left(1 - \sqrt{A}\right)^2$, one has,*

(i) *there exists a $k_0 > 0$ such that for $|k - \frac{x_Q}{y_Q}| < k_0$, system (5) has exactly two positive equilibria Q^* and E_2^* in the small neighborhood of Q and E_2, respectively, and $Q^* \to Q$ and $E_2^* \to E_2$ as $(\varepsilon, k) \to (0, \frac{x_Q}{y_Q})$. Furthermore, there exists a singular Hopf bifurcation curve $k = k_H(\sqrt{\varepsilon})$ such that Q^* is stable for $k > k_H(\sqrt{\varepsilon})$ and unstable for $k < k_H(\sqrt{\varepsilon})$. Additionally, the singular Hopf bifurcation is supercritical if $B < 0$ and subcritical if $B > 0$.*
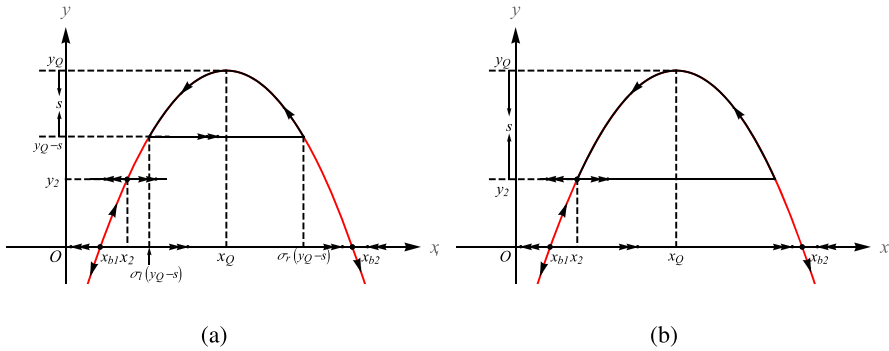
Fig. 2 The critical manifold C_2. Double arrows indicate fast flow, and single arrows indicate slow flow. **a** The sketch of the canard cycles for system (5). **b** The sketch of the homoclinic orbit for system (5)

(ii) *there exists a parameterized smooth family $s \to (k(s, \sqrt{\varepsilon}), \gamma(s, \sqrt{\varepsilon}))$ of periodic orbits bifurcated from the slow–fast cycles $\gamma(s)$ for each $s \in (0, y_Q - y_2)$ and $\gamma(s, \sqrt{\varepsilon}) \to \gamma(s)$ as $\varepsilon \to 0$, where $\gamma(s)$ (see Fig. 2a) is defined by*

$$\gamma(s) = \left\{ (x, C(x)) | x \in [\sigma_l(y_Q - s), \sigma_r(y_Q - s)] \right\} \cup \left\{ (x, y_Q - s) | x \right.$$
$$\left. \in [\sigma_l(y_Q - s), \sigma_r(y_Q - s)] \right\}, \text{ for } s \in (0, y_Q - y_2).$$

Furthermore, for $\delta \in (0, 1)$ and $s \in [\varepsilon^\delta, y_Q - y_2 - \varepsilon^\delta]$, the canard explosion occurs, where

$$\left| k(s, \sqrt{\varepsilon}) - k_c(\sqrt{\varepsilon}) \right| \le e^{-1/\varepsilon^{1-\delta}}.$$

(iii) *there exists one homoclinic orbit to the saddle E_2 for system (5) if $k = k_c(\sqrt{\varepsilon})$.*

Proof According to Theorems 3.1 in [34], for $0 < \varepsilon \ll 1$, there exists $\lambda_0 > 0$ such that for $|\lambda| < \lambda_0$, system (5) has two positive equilibria Q^* and E_2^* in the small neighborhood of Q and E_2, respectively, and $Q^* \to Q$ and $E_2^* \to E_2$ as $(\varepsilon, k) \to (0, \frac{x_Q}{y_Q})$. Furthermore, there exists a singular Hopf bifurcations curve $\lambda = \lambda_H(\sqrt{\varepsilon})$ such that Q^* is stable for $\lambda < \lambda_H(\sqrt{\varepsilon})$ and unstable for $\lambda > \lambda_H(\sqrt{\varepsilon})$. Now we show that $\frac{d\lambda}{dk} < 0$ for k sufficiently close to $\frac{x_Q}{y_Q}$. It follows from $\lambda = \frac{x_Q^{5/2}(\beta+x_Q)(x_Q-ky_Q)(\alpha+A+\beta+3x_Q-1)}{\sqrt{y_Q}(A+x_Q)(ky_Q(2\beta+x_Q)-\beta x_Q)^{3/2}}$ in (17) that

$$\frac{d\lambda}{dk} = \frac{\sqrt{y_Q} x_Q^{5/2}(\beta + x_Q)(\alpha + A + \beta + 3x_Q - 1)\left(ky_Q(2\beta + x_Q) - x_Q(4\beta + 3x_Q)\right)}{2(A + x_Q)(ky_Q(2\beta + x_Q) - \beta x_Q)^{5/2}}$$

$$= \frac{\sqrt{y_Q} x_Q^{5/2}(\beta + x_Q)(\alpha + A + \beta + 3x_Q - 1)\left((ky_Q - x_Q)(2\beta + x_Q) - 2x_Q(\beta + x_Q)\right)}{2(A + x_Q)(ky_Q(2\beta + x_Q) - \beta x_Q)^{5/2}}$$

$$< 0,$$

for k sufficiently close to $\frac{x_Q}{y_Q}$, which indicates that equation $\lambda = \frac{x_Q^{5/2}(\beta + x_Q)(x_Q - k y_Q)(\alpha + A + \beta + 3x_Q - 1)}{\sqrt{y_Q}(A + x_Q)(k y_Q(2\beta + x_Q) - \beta x_Q)^{3/2}}$ has a unique solution $k_H(\sqrt{\varepsilon})$ such that $\lambda < \lambda_H(\sqrt{\varepsilon})$ (resp. $\lambda > \lambda_H(\sqrt{\varepsilon})$) if and only if $k > k_H(\sqrt{\varepsilon})$ (resp. $k < k_H(\sqrt{\varepsilon})$). Therefore, up to now, we have established the statements (i) and (ii) by exploiting the results in [34]. Now we turn to the statement (iii), according to Theorem 3.2 in [34] (or Theorem 3.1) in [37], $C_{2,\varepsilon}^r$ will connect to $C_{2,\varepsilon}^a$ transversally if $k = k_c(\sqrt{\varepsilon})$, which implies that one of the local stable manifold E_2^s and the local unstable manifolds $E_2^{u,r}$ of E_2 are connected, and hence the homoclinic orbit follows (see Fig. 2b). The proof is completed.   □

Canard cycles in Theorem 2 indicate that the prey and predator can coexist in this system under certain parameters conditions about Allee effect a, the intra–specific competition intensity b, the mortality c, etc, and the prey and predator evolve in a periodic way.

Here we exploit numerical simulations to confirm the appearance of canard explosion. We first take $\epsilon = 0.00045$, $A = 0.4$, $\alpha = 0.05$, and $\beta = 1.8$, and then choose $k = 1.413512$, $k = 1.4135104$, and $k = 1.413510310114$, respectively, which yield canard cycles in Fig. 3a–c respectively.

Remark 2 In Theorem 2, the sign of B determines the properties of the singular Hopf bifurcation. Due to the complexity of B, generally we can not derive the explicit conditions on the sign of B. However, we can illustrate that $B < 0$, $B = 0$, and $B > 0$ are all possible under some suitable conditions by numerical examples. For instance, we have $B = -1.91402 < 0$ for $A = 0.5$, $\alpha = 0.03$, $\beta = 0.5$, and $k = 5.842138$; $B = 0$ for $A = 0.5$, $\alpha = 0.0425729$, $\beta = 0.5$, and $k = 7.372281$; and $B = 1.5398 > 0$ for $A = 0.5$, $\alpha = 0.05$, $\beta = 0.5$, and $k = 8.780488$.

4 Discussion

In this paper, we focused on the dynamical behaviors of a fast–slow Leslie–Gower predator–prey system with Allee effect and Holling Type II functional response. To be specific, by applying geometric singular perturbation theory, we first tranform system (3) into its slow–fast system (5), through which, we find the sufficient conditions for the existence of two positive equilibria and their location, and then we further fully detected their dynamics (see Theorem 1). It is worth mentioning that it is generally hard to find the sufficient conditions to determine whether an equilibrium point is a node or focus in many predator–prey systems (for example, see Theorem 2.3 in [38]). However, we indeed find some sufficient conditions to determine when the equilibrium point E_1 is node in Theorem 1. We further transformed system (5) into its slow–fast normal form, from which we determine the associated bifurcation curve and characterized its canard cycles and homoclinic orbit to the saddle E_2 with slow and fast segments under explicit parameters conditions (see Theorem 2). Finally, we also included numerical simulations to to highlight the theoretical results obtained.

From the results in Theorem 2, we see that the existence of canard point Q on the critical manifold C_2 is an organizing center for the complex dynamics including the
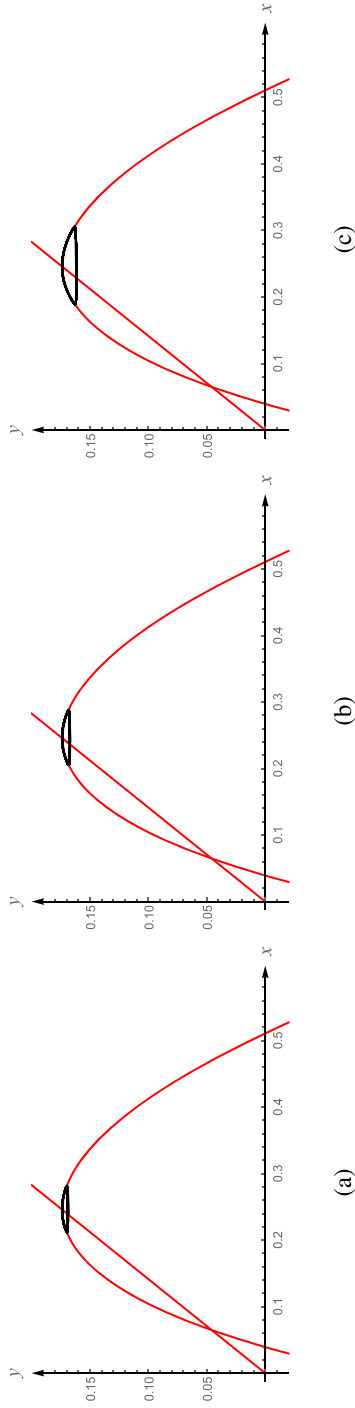
Fig. 3 Illustrations of canard cycles when $\epsilon = 0.00045$, $A = 0.4$, $\alpha = 0.05$, $\beta = 1.8$, and **a** $k = 1.413512$; **b** $k = 1.4135104$; **c** $k = 1.41351031011114$

birth of canard cycles and homoclinic orbit. From Fig. 2a or the proof of Theorem 2, canard cycles consist of fast and slow segments. The biological interpretation of this interesting feature is as follows: the existence of the canard cycle indicates that the prey and predator can coexist in this concrete system. When the predator density is lower than a certain level, we have a prey outbreak in a very short time. After the prey density arrives at some level which is enough to support the reproduction of the predators, the predator density begins to grow slowly and the prey density begins to decrease slowly for a long period. As the prey density continuous to decrease slowly, the predator density declines slowly due to the less food. After some time, the whole procedure continues and forms a periodic move.

As we know, many important factors [10–13, 15], such as functional response, Allee effect, fear effect, prey refuge, cooperation hunting and so on, determine rich and complex dynamics of prey–predator relationship. In the later study, we can consider the slow–fast dynamics of the predator–prey models including these factors and expect to find new dynamical behaviors.

Author Contributions T.S. carried out the investigation, prepared figure 1 and wrote the original draft manuscript. Z.W. convinced the study, verified the investigation and wrote the main manuscript. All authors reviewed the manuscript.

Data Availability No datasets were generated or analysed during the current study.

Declarations

Conflict of interest The authors declare no conflict of interest

References

1. Leslie, P.H.: Some further notes on the use of matrices in population mathematics. Biometrika **35**(3/4), 213–245 (1948)
2. Leslie, P.: A stochastic model for studying the properties of certain biological systems by numerical methods. Biometrika **45**(1–2), 16–31 (1958)
3. Hsu, S.B., Huang, T.W.: Global stability for a class of predator-prey systems. SIAM J. Appl. Math. **55**(3), 763–783 (1995)
4. Hsu, S.B., Hwang, T.W.: Hopf bifurcation analysis for a predator–prey system of Holling and Leslie type. Taiwan. J. Math. **3**(1), 35–53 (1999)
5. Korobeinikov, A.: A Lyapunov function for Leslie–Gower predator–prey models. Appl. Math. Lett. **14**(6), 697–699 (2001)
6. Yuan, S., Song, Y.: Bifurcation and stability analysis for a delayed Leslie–Gower predator–prey system. IMA J. Appl. Math. **74**(4), 574–603 (2009)
7. Holling, C.S.: The functional response of predators to prey density and its role in mimicry and population regulation. Mem. Entomol. Soc. Can. **97**(S45), 5–60 (1965)
8. Huang, J., Ruan, S., Song, J.: Bifurcations in a predator–prey system of Leslie type with generalized Holling type III functional response. J. Differ. Equ. **257**(6), 1721–1752 (2014)
9. Dai, Y., Zhao, Y., Sang, B.: Four limit cycles in a predator–prey system of Leslie type with generalized Holling type III functional response. Nonlinear Anal. Real World Appl. **50**, 218–239 (2019)
10. Tiwari, V., Tripathi, J.P., Mishra, S., Upadhyay, R.K.: Modeling the fear effect and stability of non-equilibrium patterns in mutually interfering predator–prey systems. Appl. Math. Comput. **371**, 124948 (2020)

11. Tripathi, J.P., Bugalia, S., Jana, D., Gupta, N., Tiwari, V., Li, J., Sun, G.Q.: Modeling the cost of anti-predator strategy in a predator-prey system: the roles of indirect effect. Math. Methods Appl. Sci. **45**(8), 4365–4396 (2022)
12. Tripathi, J.P., Abbas, S., Thakur, M.: Dynamical analysis of a prey–predator model with Beddington–DeAngelis type function response incorporating a prey refuge. Nonlinear Dyn. **80**, 177–196 (2015)
13. Tripathi, J.P., Abbas, S., Thakur, M.: A density dependent delayed predator-prey model with Beddington–DeAngelis type function response incorporating a prey refuge. Commun. Nonlinear Sci. Numer. Simul. **22**(1–3), 427–450 (2015)
14. Allee, W., Bowen, E.S.: Studies in animal aggregations: mass protection against colloidal silver among goldfishes. J. Exp. Zool. **61**(2), 185–207 (1932)
15. Tripathi, J.P., Mandal, P.S., Poonia, A., Bajiya, V.P.: A widespread interaction between generalist and specialist enemies: the role of intraguild predation and Allee effect. Appl. Math. Model. **89**, 105–135 (2021)
16. Aguirre, P., Gonzalez-Olivares, E., Sáez, E.: Two limit cycles in a Leslie–Gower predator-prey model with additive Allee effect. Nonlinear Anal. Real World Appl. **10**(3), 1401–1416 (2009)
17. Aguirre, P., González-Olivares, E., Sáez, E.: Three limit cycles in a Leslie-Gower predator-prey model with additive Allee effect. SIAM J. Appl. Math. **69**(5), 1244–1262 (2009)
18. Aguirre, P.: A general class of predation models with multiplicative Allee effect. Nonlinear Dyn. **78**(1), 629–648 (2014)
19. Zhu, Z., Chen, Y., Li, Z., Chen, F.: Stability and bifurcation in a Leslie–Gower predator–prey model with Allee effect. Int. J. Bifurc. Chaos **32**(03), 2250040 (2022)
20. Zu, J., Mimura, M.: The impact of Allee effect on a predator-prey system with Holling type II functional response. Appl. Math. Comput. **217**(7), 3542–3556 (2010)
21. Zu, J.: Global qualitative analysis of a predator-prey system with Allee effect on the prey species. Math. Comput. Simul. **94**, 33–54 (2013)
22. Wang, C., Zhang, X.: Canards, heteroclinic and homoclinic orbits for a slow–fast predator–prey model of generalized Holling type III. J. Differ. Equ. **267**(6), 3397–3441 (2019)
23. Su, W., Zhang, X.: Global stability and canard explosions of the predator–prey model with the Sigmoid functional response. SIAM J. Appl. Math. **82**(3), 976–1000 (2022)
24. Chen, X., Zhang, X.: Dynamics of the predator-prey model with the Sigmoid functional response. Stud. Appl. Math. **147**(1), 300–318 (2021)
25. Atabaigi, A.: Canard explosion, homoclinic and heteroclinic orbits in singularly perturbed generalist predator–prey systems. Int. J. Biomath. **14**(01), 2150003 (2021)
26. Saha, T., Pal, P.J., Banerjee, M.: Slow-fast analysis of a modified Leslie–Gower model with Holling type I functional response. Nonlinear Dyn. **108**(4), 4531–4555 (2022)
27. Zhu, Z., Liu, X.: Canard cycles and relaxation oscillations in a singularly perturbed Leslie–Gower predator-prey model with Allee effect. Int. J. Bifur. Chaos **32**(05), 2250071 (2022)
28. Zhao, L., Shen, J.: Canards and homoclinic orbits in a slow–fast modified May–Holling–Tanner predator-prey model with weak multiple Allee effect. Discrete Contin. Dyn. Syst. B **27**(11), 6745–6769 (2022)
29. Shi, T., Wen, Z.: Canard cycles and their cyclicity of a fast–slow Leslie–Gower predator–prey model with Allee effect. In: International Journal of Bifurcation and Chaos, accepted
30. Chowdhury, P.R., Banerjee, M., Petrovskii, S.: Canards, relaxation oscillations, and pattern formation in a slow–fast ratio-dependent predator-prey system. Appl. Math. Model. **109**, 519–535 (2022)
31. Li, K., Li, S., Wu, K.: Relaxation oscillations and canard explosion of a Leslie–Gower predator-prey system with addictive Allee effect. Int. J. Bifurc. Chaos **32**(11), 2250168 (2022)
32. Wen, Z., Shi, T.: Existence and uniqueness of a canard cycle with cyclicity at most two in a singularly perturbed Leslie-Gower predator-prey model with prey harvesting. Int. J. Bifurc. Chaos **34**(03), 2450036 (2024)
33. Fenichel, N.: Geometric singular perturbation theory for ordinary differential equations. J. Differ. Equ. **31**(1), 53–98 (1979)
34. Krupa, M., Szmolyan, P.: Relaxation oscillation and canard explosion. J. Differ. Equ. **174**(2), 312–368 (2001)
35. Kuznetsov, Y.A., Muratori, S., Rinaldi, S.: Homoclinic bifurcations in slow–fast second order systems. Nonlinear Anal. Theory Methods Appl. **25**(7), 747–762 (1995)
36. Shen, J.: Canard limit cycles and global dynamics in a singularly perturbed predator–prey system with non-monotonic functional response. Nonlinear Anal. Real World Appl. **31**, 146–165 (2016)

37. Krupa, M., Szmolyan, P.: Extending geometric singular perturbation theory to nonhyperbolic points–fold and canard points in two dimensions. SIAM J. Math. Anal. **33**(2), 286–314 (2001)
38. Lu, M., Huang, J.: Global analysis in Bazykin's model with Holling II functional response and predator competition. J. Differ. Equ. **280**, 99–138 (2021)